Far Ultraviolet and Hα Imaging of Nearby Spirals: The OB Stellar Population in the Diffuse Ionized Gas

Charles G. Hoopes[1], René A. M. Walterbos[2,3], & Gregory D. Bothun[4]

ABSTRACT

We have compared Hα and far ultraviolet (FUV) images of 10 nearby spirals, with the goal of understanding the contribution of field OB stars to the ionization of the diffuse ionized gas (DIG) in spiral galaxies. The FUV images were obtained by the Ultraviolet Imaging Telescope (UIT) and the Hα images were obtained using various ground-based telescopes. In all of the galaxies, the $F_{H\alpha}/F_{UIT}$ flux ratio is lower in the DIG than in the H II regions. This is likely an indication that the mean spectral type for OB stars in the field is later than that in H II regions. Comparison of the N_{Lyc}/L_{UIT} ratio with models of evolving stellar populations shows that the stellar population in the DIG is consistent with either an older single burst population or a steady state model with constant star formation and an initial mass function (IMF) slope steeper than $\alpha=2.35$. The steady state model is probably a more realistic representation of the stellar population outside of H II regions. The steep IMF slope simulates the steep present-day mass function slope expected for field OB stars, and does not necessarily indicate that IMF slope is actually steeper than $\alpha=2.35$. We compared the $F_{H\alpha}/F_{UIT}$ ratio in the DIG of these galaxies with that in M33, in which the field OB stellar population has previously been investigated using Hubble Space Telescope images. If the mean spectral types of stars in H II regions and in the DIG are the same as in M33, and the difference in extinction between DIG and H II regions is constant among galaxies, then the analysis suggests that field stars are important sources of ionization in most galaxies, and may be the dominant source in some galaxies.

[1]Department of Physics and Astronomy, Johns Hopkins University, 3400 North Charles Street, Baltimore, MD 21218; choopes@pha.jhu.edu

[2]Department of Astronomy, New Mexico State University, MSC 4500, Box 30001, Las Cruces, New Mexico 88003; rwalterb@nmsu.edu

[3]Visiting Astronomer, Kitt Peak National Observatory and Cerro-Tololo Inter-American Observatory, National Optical Astronomy Observatories, operated by the Association of Universities for Research in Astronomy, Inc. (AURA) under cooperative agreement with the National Science Foundation.

[4]Physics Department, University of Oregon, Eugene, OR 97403; nuts@bigmoo.uoregon.edu

The $F_{H\alpha}/F_{UIT}$ ratio is correlated with Hα surface brightness in both DIG and H II regions, although there is a large scatter in faint H II regions, which may be due to undersampling the IMF in regions with a low total mass of stars formed. The $F_{H\alpha}/F_{UIT}$ ratio is often highest in the centers of galaxies and in the spiral arms, which is also where the DIG is brightest. This can be explained if the extinction is greater in these regions, or if the fraction of DIG ionized by leakage is lower in the inter-arm regions.

Subject headings: galaxies: individual (M33, M51, M81, M74, M101, NGC 1313, NGC 1566, NGC 1512, NGC 925, NGC2903) — galaxies: ISM — ultraviolet: galaxies

1. Introduction

The details of the relationship between massive stars and the ISM are crucial to understanding how galaxies evolve. One place where this interaction is critical, and not well understood, is in the diffuse ionized gas (DIG). This is the dominant component of ionized gas in terms of mass, contributing 95% of the ionized gas mass in the Milky Way (Reynolds 1991), and requiring the equivalent of 30 to 50% of the ionizing photons of OB stars to remain ionized in almost all of the external spirals studied (Walterbos & Braun 1996). The DIG is clearly an important physical manifestation of energy transfer from stars to gas, yet the mechanisms through which this transfer occurs remain unclear. The large energy requirement, the morphological association of DIG with H II regions (Walterbos & Braun 1994; Ferguson et al. 1996; Hoopes, Walterbos, & Greenawalt 1996; Greenawalt 1998; Greenawalt et al. 1998), and the spectral properties of the DIG (Greenawalt, Walterbos, & Braun 1997; Wang et al. 1997; Galarza, Walterbos, & Braun 1999; Haffner, Reynolds, & Tufte 1999) all very strongly suggest OB stars as the ionization source, although there are indications that other sources, such as old supernova remnants (Slavin, McKee, & Holenbach 2000) or turbulent mixing layers (Slavin, Shull, & Begelman 1993) also play a role (Wang et al. 1997). However, problems transporting the ionizing photons from OB stars to the DIG remain unsolved. Specifically, if the ionizing stars are in H II regions, are there enough density-bounded H II regions leaking ionizing photons, as well as paths through the H I in spiral disks, for these photons to reach the DIG?

An alternative is that field OB stars ionize some of the DIG, reducing the amount of leakage from H II regions required. Field OB stars have been studied in the Milky Way (Torres-Peimbert, Lazcano-Araujo, & Peimbert 1974), the Magellanic Clouds (Massey et al. 1995b), and M33 (Patel & Wilson 1995; Hoopes & Walterbos 2000). There are several

possible explanations for the presence of these OB stars outside of H II regions. They may form in H II regions, but then diffuse out of the H II region into the diffuse gas, or they may survive as an H II region is destroyed by supernovae (SNe) from other massive stars. Both of these processes would produce a population in the field that is weighted toward later-type ionizing stars. A late-type (B0-O9) ionizing star has a longer lifetime than an earlier-type star, increasing the probability that it will live long enough to move an appreciable distance from its birthplace, or survive as the H II region is destroyed when the more massive stars explode in SNe. Another possibility is that field OB stars actually form in the field, as suggested by Massey et al. (1995b) for the Magellanic Clouds. Those authors defined their sample of field stars so that it would not include stars which might have traveled out of an H II region. However, they also found that the initial mass function (IMF) for field stars has a steeper slope than in H II regions, making the very early-type OB stars rare. All of these mechanisms, then, lead to a field population dominated by later-type OB stars. These stars must ionize some fraction of the DIG, but since they are predominantly later-types, a large number is needed to explain all of the DIG. The presence of just one O3 star in the field is equivalent to 50 B0 stars.

A direct way to determine the fraction of DIG that is ionized by field OB stars is to look for OB stars in and out of H II regions, determine their spectral types and ionizing luminosities (N_{Lyc}), and compare this to the energy required to maintain the observed Hα luminosity. This was done for H II regions in the LMC, and several were found that may be leaky (Oey & Kennicutt 1997). Hoopes & Walterbos (2000) studied OB stars in H II regions and DIG in M33, using *Hubble Space Telescope* (HST) far-ultraviolet (FUV) and optical images. The FUV information is crucial for assigning ionizing luminosities to massive stars, as there is a severe color degeneracy for hot stars at optical wavelengths (Massey 1985; Massey et al. 1995a). Even in the FUV the color degeneracy is a problem, but when combined with the FUV and optical absolute magnitudes, the problem is reduced to a level where values of N_{Lyc} good to the equivalent of about ±1 spectral subtype can be obtained.

The current paper builds on the results of Hoopes & Walterbos (2000), so we briefly describe the analysis carried out in that paper. The goal was to determine the ionizing luminosities of stars in H II regions and in the field, in order to compare with ionizing luminosity inferred from the Hα emission in each environment. Magnitudes were measured from the WFPC2 images in four filters, F170W, F336W, F439W, and F555W, along with the statistical uncertainty and flat fielding uncertainty, for each star. Color magnitude diagrams (CMDs) for each H II region and DIG region were plotted and compared to theoretical CMDs (Schaerer, et al. 1993). The extinction correction required to place the observed main sequence on the theoretical main sequence was then determined, resulting in a mean extinction correction for each region. A conservative estimate of the uncertainty in determining

this correction was combined with the previously measured uncertainty in the photometry.

The extinction corrected magnitudes in four bands for all of the stars were compared with the predicted magnitudes for massive stars from the CoStar models (Schaerer & de Koter 1997), and N_{Lyc} from the best matching model was assigned to each star. The uncertainty in N_{Lyc} was determined by finding the models with the largest and smallest ionizing luminosities that matched within the 1σ uncertainty in the magnitudes (which included statistical, flat-field, and extinction uncertainties). The N_{Lyc} values for all stars in a given H II region or DIG region were summed together, and compared with N_{Lyc} required by the Hα emission. In the regions of M33 that were investigated, OB stars outside of H II regions can ionize an appreciable amount of the DIG, $40\% \pm 12\%$, while the OB stars in H II regions account for $107\% \pm 26\%$ of the observed Hα luminosity of the H II regions. The good agreement between the mean predictions and observations for H II regions gives confidence that the DIG result is not affected by systematic uncertainties. Thus, even though estimates of ionizing luminosities for individual stars have substantial uncertainty since spectral classification from photometry alone is not very accurate, the overall result seems robust. The sizable contribution of field OB stars to the ionization of the DIG relaxes somewhat the need for leaky H II regions, and emphasizes the fact that OB stars outside of H II regions have a large impact on the ISM.

In this paper we investigate whether the source of the DIG ionization in M33 is similar to other spirals. In more distant spirals HST cannot resolve individual stars. We have used images acquired by the *Ultraviolet Imaging Telescope* (UIT) to yield global FUV information, which can then be compared to M33, in which we have both HST and UIT data. The resolution of the UIT images is approximately $2''$ or ~ 80 parsecs at the typical distances of our targets. Thus we can well resolve the FUV field. Comparing the spatial distribution of FUV emission to that of the H II regions (from narrow band Hα imaging) in our target galaxies will allow for an assessment of the sources of ionization in a manner similar to that done by Hoopes & Walterbos (2000).

2. Data Reduction and Analysis

The sample of galaxies for which we analyzed Hα and FUV images is described in Table 1. Ten galaxies were included, including M33 which was studied previously (Hoopes & Walterbos 2000). The sample spans a range of Hubble types, but early-type spirals are under represented. Most of the galaxies are nearby, although NGC 1512 and NGC 1566 are beyond 15 Mpc. A metallicity estimate for each galaxy was taken from Zaritsky et al. (1994), using their value of 12+log(O/H) at a radius of 3 kpc from the nucleus.

Table 2 summarizes the Hα data for each galaxy. The reduction for M33 was described in Greenawalt (1998) and Hoopes & Walterbos (2000), M81 and M51 were discussed in Greenawalt et al. (1998), and M101, NGC 628, NGC 925, and NGC 2903 were discussed in Greenawalt (1998). Both line and nearby continuum images were obtained, and the continuum image was scaled to the line image by comparing the fluxes of foreground stars, and then subtracted to produce a line-only image. The calibration method for each galaxy is given in Table 2. Most were calibrated using observations of a standard star, but a few were calibrated using the R-band magnitude of the galaxy and the shape of the narrow band filter, and a few were calibrated by comparing the luminosities of specific H II regions to published values. Three galaxies, NGC 3031 (M81), NGC 5194 (M51) and NGC 5457 (M101) were observed through Hα filters wide enough to include a contribution from [N II] $\lambda 6548 + 6584$ Å. In these cases, 20 to 30% of the luminosity my arise from [N II]. We have not corrected for this contamination, but it will be addressed in the relevant sections.

Table 3 summarizes the UIT data for the sample. Details of the UIT instrument and data characteristics can be found in Stecher et al. (1997). The UIT instrument was flown on two occasions: the Astro-1 mission aboard the space shuttle Columbia in December, 1990, and the Astro-2 mission aboard the space shuttle Endeavor in March, 1995. The galaxies were observed by the FUV (~ 1500Å) camera, through one of two filters: B1 (1520Å, $\Delta \lambda$ 354Å) and B5 (1615Å, $\Delta \lambda$ 225Å). The images were originally produced on film, and later digitized on the ground. The images were calibrated by observing standards stars observed previously with the International Ultraviolet Explorer, and are estimated to be accurate to 15% (Stecher et al. 1997). Nonlinearity at low flux levels introduces further uncertainty. The effects of nonlinearity have been found to be as high as 20%, and the effects vary significantly between exposures (Bell & Kennicutt 2001). We adopt 15% uncertainty for H II region UIT flux, and 25% (15% + 20% in quadrature) for the fainter DIG UIT flux. The UIT images have an angular resolution of about 2″.

For each galaxy the DIG was isolated in the Hα image using the masking procedure described in Hoopes, Walterbos, & Greenawalt (1996). The Hα image was smoothed with a median filter using a linear length scale of 1 kpc. The smoothed version was subtracted from the original, leaving an image of the small scale structure only, the smoothly varying component having been subtracted away. On this image a mask was created by replacing pixels with values less than 50 pc cm^{-6} in emission measure with one, and pixels with values greater than 50 pc cm^{-6} with zero. The resulting mask thus has a value of zero in the bright, small scale structures (*i.e.* H II regions), and one everywhere else. The original (unsmoothed) Hα image was then multiplied by the mask image, leaving an image of only the DIG, with zeros over the H II regions. This is called the DIG Hα image. A DIG FUV image was also created by multiplying the FUV image with the same mask (the mask defined on the

Hα image). An H II region mask was created by inverting the DIG mask, and this was multiplied with the Hα and FUV images, producing an H II region Hα image and an H II region FUV image.

Using the H II region Hα image, circular apertures were defined by eye for as many H II regions as possible. The fluxes of these regions were then measured on the original (unmasked) Hα and FUV images. The H II region image is used only to find the H II regions with no confusion from the DIG. A local background was defined for each H II region as the mode of the pixel values in an annulus around the aperture. This background was subtracted from each pixel in the aperture.

The DIG fluxes were measured in square $500{\times}500$ pc apertures which covered the galaxy. The fluxes were measured on the DIG images with the H II regions masked out. A lower cutoff equal to the 1-σ noise level in the Hα image was applied to the resulting images, in order to remove apertures which did not include any DIG. For each galaxy there were a small number of apertures that contained Hα flux but no FUV flux (both DIG and H II regions after background subtraction). These were not included in the final analysis. These procedures follow exactly those used to analyze M33 in Hoopes & Walterbos (2000).

3. Results

3.1. The Hα/FUV Ratio

In Table 4 we list the observed Hα and FUV properties of the sample galaxies. The global $F_{H\alpha}/F_{UIT}$ DIG and H II region ratios were measured using the masked images. The diffuse fraction is the ratio of the DIG Hα luminosity (measured on the masked DIG image) to the total Hα luminosity of the galaxy. The FUV diffuse fraction is the fraction of the total FUV luminosity that arises in the DIG. The uncertainty in $L_{H\alpha}$ and in the Hα diffuse fraction was found by varying the continuum scale factor by $\pm3\%$. The uncertainty in the flux ratios is the combination of the uncertainty in $L_{H\alpha}$ and the uncertainty in L_{UIT}, which is the 15% calibration uncertainty in HII regions, and 25% (15% calibration and 20% nonlinearity) in DIG (Stecher et al. 1997; Bell & Kennicutt 2001). For the ratio of total luminosities we conservatively use the 25% uncertainty for L_{UIT}. In all cases except NGC 1512, the Hα diffuse fraction is roughly between 30 and 50%. The Hα/FUV ratios are higher in the DIG than in H II regions. This can also be seen in the FUV diffuse fraction, which is much higher than the Hα diffuse fraction for all of the galaxies. In the FUV, a greater fraction of light is found in the field than in Hα, due to the fact that the FUV band includes light from later-type B and A stars. In NGC 1512, 39% of the Hα flux is emitted by the

nuclear star-forming ring. If this region is excluded, the Hα diffuse fraction rises to about 20%.

Figure 1 shows the histograms of the $F_{H\alpha}/F_{UIT}$ flux ratio for the galaxies observed in the B1 filter, and Figure 2 shows the galaxies observed through the B5 filter. The histograms show the observed values; no correction for extinction has been made at this point. M33 is shown twice because it was observed through both the B1 and B5 filters. The three galaxies with [N II] contamination are not noticeably different, but the correction to the ratio would be only about 0.1 in the logarithmic plots.

In all of the galaxies in the sample, H II regions have a higher $F_{H\alpha}/F_{UIT}$ ratio than DIG regions. Hoopes & Walterbos (2000) interpreted this trend seen in M33 as a hotter stellar population in the H II regions, and confirmed the interpretation through HST WFPC2 imaging of individual OB stars in H II regions and DIG. The Hα emission results from ionizing photons, so the $F_{H\alpha}/F_{UIT}$ ratio is really a ratio of ionizing/non-ionizing UV photons. The spectra of hotter stars will have a higher ratio of ionizing to non-ionizing photons (*i.e.* a *bluer* spectrum) than that of cooler stars. The difference suggests that the population of ionizing stars in the field is dominated by cooler, later-type OB stars, in qualitative agreement with the mechanisms for forming field stars discussed in section 1.

3.2. Comparison with Starburst99 Models

In this section we compare the $F_{H\alpha}/F_{UIT}$ ratios to models of evolving stellar populations, to see whether the observed ratios can be reproduced by a reasonable population of stars. Figures 3 and 4 show the same histograms as Figures 1 and 2, but now they are shown sideways for comparison with the models. We have also converted the Hα luminosity to the number of ionizing photons N_{Lyc}, assuming case B recombination (Osterbrock 1989) and neglecting absorption of ionizing photons by dust. The histograms now include a rough extinction correction, which depends upon the models also shown in the figures. First we will describe the models, and then we will describe the correction for extinction.

The Starburst99 stellar population evolution model (Leitherer et al. 1999) was used to simulate the conditions in H II regions and in the field. This model simulates the evolution of a star cluster through time, and allows one to change parameters, such as the initial mass function (IMF), metallicity, and star formation rate. We ran two types of models. One set has a single burst of star formation, which represent an H II region. The other is a steady state model with constant star formation, which roughly approximates the conditions in the field, in which a relatively small population of young stars is superimposed on a much larger

population of old stars.

The burst models begin with a high N_{Lyc}/L_{UIT} ratio, as the cluster is dominated by hot young stars with large ionizing luminosities. As the cluster ages and the most massive stars evolve and die, N_{Lyc} drops, while L_{UIT} stays relatively constant since it contains emission from later-type B stars as well as O stars, so the N_{Lyc}/L_{UIT} ratio falls. Thus the N_{Lyc}/L_{UIT} ratio is a good indicator of the age of a burst population (Hill et al. 1995, 1998; Stewart et al. 2000). The steady state models reach an equilibrium value.

The metallicity of each type of model was varied to include LMC like abundances(z=0.08), solar (z=0.20) and twice solar (z=0.40). The metallicity chosen for each galaxy was based on the measurements of Zaritsky et al. (1994) in Table 1. We also varied the IMF slope to include α=2.35, 3.00. and 3.50. The purpose was to simulate a steeper mass function slope, which might arise from the processes which that produce field OB stars (see section 1). The steeper mass function results in a lower N_{Lyc}/L_{UIT} ratio, as the most massive O stars become rare compared to the number of less massive OBA stars. For H II regions we show only the standard α=2.35 IMF models, as there has been no indication of variation of the IMF in H II regions (Massey 1998).

In order to make a rough estimate of the extinction in each galaxy, we assume that the single burst models are appropriate for the brightest H II regions in each galaxy (*e.g.* von Hippel & Bothun 1990). The brightest regions probably have the largest number of O stars, and thus the IMF is more likely to be well sampled. Under-sampling the IMF can have a large effect on the N_{Lyc}/L_{UIT} ratio, and this is likely to happen if the number of O stars is low. An extreme case is a single O3 star and no other UV emitting stars, resulting in a very high N_{Lyc}/L_{UIT} ratio. This is why we do not use the H II regions with the highest observed N_{Lyc}/L_{UIT} to define the extinction correction, as one might be tempted to do since the models predict that these should be the youngest H II regions.

For each galaxy we found the average of log N_{Lyc}/L_{UIT} for the ten brightest H II regions (only 3 for M33, which lacks very bright H II regions). The average value was compared to the prediction of the single burst model (for the metallicity of that galaxy) at 1 Myr. We chose this age based on the assumption that part of the reason these H II regions are bright is that they are young, since the models in Figures 3 and 4 show that after a few Myr the ionizing luminosity of a star cluster drops drastically as the most massive stars die. The difference between the mean log N_{Lyc}/L_{UIT} and the model value is the extinction correction for that galaxy. The histograms in Figures 3 and 4 have been corrected by that amount. Table 5 lists the shifts used for each galaxy, and the corresponding E(B-V) for two extinction laws. Since the magnitude of the correction was measured, the particular extinction law does not matter, but the values are shown for reference. Published values of E(B-V) for these

galaxies are also listed in Table 5.

Correcting for extinction moves the histograms down in the plots, because the correction for L_{UIT} is larger than that for N_{Lyc} (measured through Hα). We do not specifically correct the ionizing photon flux for absorption by dust, however making the H II regions equal to the model predictions should also correct for this. McKee & Williams (1997) find that about 25% of the ionizing photons emitted by stars in H II regions are absorbed by dust. The effect of absorption by dust on the observed histograms is to move them down, by making the N_{Lyc}/L_{UIT} lower, so the correction for this works in the opposite sense of correcting the Hα and FUV light for extinction. This may be part of the reason that the extinction values in Table 5 are lower than the previously determined values for those galaxies.

This is an average correction for all H II regions (and DIG). Part of the scatter in the histogram is probably due to differences in extinction from region to region, but we have no way to correct for this. A large assumption in this process is that the extinction in the DIG is the same as that for H II regions. In reality it is likely that the extinction is somewhat different due to several processes, an example being the destruction of large grains due to shocks in H II regions (Jones, Tielens & Hollenbach 1996). In both M31 (Greenawalt, Walterbos, & Braun 1997) and M33 (Hoopes & Walterbos 2000) the difference has been small, about ΔA_V=0.3. This much difference would move the DIG histograms in Figures 3 and 4 up by 0.22 using the Milky Way extinction law, and 0.32 using the LMC extinction law. It is also possible that the fraction of N_{Lyc} absorbed by dust is different in the DIG. We will discuss the effects of a difference in extinction where it is relevant.

The extinction corrections for NGC 1313, NGC 1512, NGC 1566, and NGC 925, are particularly low. These are also the four galaxies (besides M33) that were observed through the B5 filter. The extinction correction derived for the two M33 observations are remarkably consistent, so there does not seem to be a problem with the B5 filter. There may be a calibration problem with the FUV images of these galaxies, or there may be a real difference between these and the other galaxies, such as a higher fraction of N_{Lyc} absorbed by dust. In any case, the results for these galaxies should be treated with caution.

After the extinction correction, most of the galaxies look very similar to M33. The DIG ratios are consistent with a steady state model, or with a single burst model older than that for H II regions. The steady state model seems like a more realistic model for the field stellar population than an older burst, as the steady state model represents a disk built up through star formation over several Gyr, with a much smaller population of young stars. The DIG histograms exhibit even better agreement with the steady state models with somewhat steeper IMF slopes, which was also seen in M33. As already stated, the steep IMF slopes in the models simulate a steep *present-day* mass function slope, which may be a result of the

way H II region stars become field stars, and not necessarily an indication of how field stars actually form.

3.3.   Analysis of the Observed Ratios

The comparison with the Starburst99 models supports the general conclusion that the field OB star populations in these galaxies are similar to that in M33, and that they are likely to ionize a similar fraction of the DIG. However, the differences that do exist between these galaxies may indicate real differences in the amount of leakage or field star ionization present. A comparison of the mean $F_{H\alpha}/F_{UIT}$ ratios may elucidate some of these differences or lack thereof. Instead of comparing to models, we will compare the observed $F_{H\alpha}/F_{UIT}$ ratios to those seen in M33, where we have independent information on the fraction of DIG ionized by field OB stars. In this section we use only the observed values, without the extinction correction described in the last section.

The analysis is complicated by the important effects of extinction at ultraviolet wavelengths, and the possible differences in stellar populations in the field and in H II regions due to varying star formation histories, metallicity, or IMF slopes. To mitigate these complicating factors, we will begin the analysis by making some simplifying assumptions. First we will assume that the H II region stellar population is the same among galaxies. This means that the mean intrinsic $F_{H\alpha}/F_{UIT}$ ratio in H II regions for all of the galaxies will be the same. The variation seen in the observed ratio (Table 5) is within the range that can be explained by differences in the amount of extinction, so we have no evidence that this assumption is false. Second, we assume that the relative extinction in H II regions and DIG is the same for all galaxies. By relative, we mean that there may be more or less extinction in DIG compared to H II regions, but the difference between H II region and DIG extinction will be constant for all galaxies. For M31 and M33, the only two galaxies where this has been measured, this assumption appears to be true (Greenawalt, Walterbos, & Braun 1997; Hoopes & Walterbos 2000).

With these assumptions we can then use the measured H II region ratio to anchor the DIG ratio, independent of extinction. The difference between the H II region ratio and the DIG ratio can then be compared among galaxies. This approach does not suffer from the effects of any errors that might have been made in the extinction correction made using the starburst models. Table 6 lists for each galaxy the differences in the logarithm of the mean observed $F_{H\alpha}/F_{UIT}$ ratios for H II and DIG. If the assumptions we have made are true, then the difference in this value for different galaxies is completely due to a difference in the $F_{H\alpha}/F_{UIT}$ ratio in the DIG, since we have assumed that the H II ratio is constant, and the

H II/DIG relative comparison removes the effects of extinction.

The interpretation of these values is still complicated. Since the H II regions are ionized by local stars with no leakage of ionizing photons into the system, the simplest interpretation is to consider them as the zero-leakage reference point for the DIG. In this case differences between the H II region and DIG ratios would be interpreted as being due to leakage, with larger differences indicating more leakage. However, all of the DIG $F_{H\alpha}/F_{UIT}$ ratios are smaller than the H II region ratios. The largest differences arise from the smallest DIG ratios, so taking this scenario to the extreme means that a ratio of zero (*i.e.* no Hα emission) corresponds to maximum leakage. The key point is that leakage should always increase the $F_{H\alpha}/F_{UIT}$ ratio in the DIG by adding Hα flux but no FUV flux. Since the DIG ratios are always lower than the H II region ratios, leakage cannot be the only factor affecting the ratios.

The other factor is the stellar population in the field, which is different from that in H II regions. Hoopes & Walterbos (2000) found that the mean spectral type of stars in the field is later than that in H II regions, a conclusion also found for the LMC, SMC, and Milky Way (Massey et al. 1995b). Later type stars have lower ratios of L_{Lyc}/FUV luminosity (*i.e.* more FUV luminosity relative to their ionizing luminosity). This results in lower $F_{H\alpha}/F_{UIT}$ ratio for DIG than H II regions in the absence of leakage. Because of this fact, H II regions do not represent the zero-leakage reference point for DIG.

However, we can use the M33 ratio as a reference point for the DIG in other galaxies, since we know that field OB stars ionize $\sim 40\%$ of the DIG in that galaxy (Hoopes & Walterbos 2000). Table 6 shows the difference in the $F_{H\alpha}/F_{UIT}$ ratio relative to M33. Here we make another assumption: the mean spectral type of the field stars, while different from that in H II regions, is the same in all of the galaxies. Then the difference in the ratio can be understood as being due solely to a difference in the fraction of DIG ionized by leakage. The $F_{H\alpha}/F_{UIT}$ ratio for the DIG that is ionized only by field stars remains the same, independent of the number of field stars, since the mean spectral type is constant. Then any change in the DIG $F_{H\alpha}/F_{UIT}$ ratio is caused by the addition or subtraction of Hα flux from DIG ionized by leakage.

We illustrate this scenario using M51 as an example. The observed difference in the mean log $F_{H\alpha}/F_{UIT}$ ratio for DIG and H II regions for M51 is 1.09, while for M33 it is 0.81. Since this is a difference of logarithms it is actually a ratio, and if the intrinsic H II region $F_{H\alpha}/F_{UIT}$ ratios are the same for both galaxies, this difference means that the M51 $F_{H\alpha}/F_{UIT}$ ratio for DIG is 0.52 that in M33. We assume that this difference is totally due to a change in the fraction of DIG ionized by leakage. In M33, 40% of the DIG is ionized by field stars, so 60% of the observed Hα in the DIG come from leakage. The Hα flux from

leakage in M51 has to be reduced to get the lower observed $F_{H\alpha}/F_{UIT}$ ratio, resulting in a fraction of DIG ionized by leakage of 23%, and 77% ionized by field OB stars. The fraction of DIG ionized by field stars for each galaxy based on these assumptions is shown in Table 6.

In this scenario, field OB stars dominate the ionization of the DIG in M51 and NGC 628, NGC 1313 and NGC 1512 have smaller contributions from field stars, and the other galaxies are similar to M33. The large Hα luminosities of M51 and NGC 628 indicate that they have both undergone recent galaxy-wide star formation events. If this is connected with the dominance of the field OB stars, it suggests that these events somehow enhance the creation of field OB stars, but do not affect the amount of DIG ionized by leakage. This is highly speculative however, since other galaxies in the sample have had recent star formation, but do not appear to exhibit this effect. The Hα filter used for M51 contains a contribution from [N II], and the [N II]/Hα ratio is higher in the DIG, which may affect the observed difference. However, correcting for this would make the $F_{H\alpha}/F_{UIT}$ ratio lower in the DIG compared to H II regions, and make the difference between H II regions and DIG even larger, raising the predicted contribution of field OB stars even higher.

If the assumption that the field star populations are similar in spectral type in all galaxies is in error, the analysis becomes more complicated. In this case the $F_{H\alpha}/F_{UIT}$ ratio for DIG ionized by field stars will be different, higher in galaxies where the mean spectral type is earlier, and lower if the mean spectral type is later. Put another way, if the mean spectral type is earlier, then a field star population with a given amount of FUV luminosity can ionize more DIG (resulting in higher Hα luminosity) than in a galaxy with a later mean spectral type in the field. The $F_{H\alpha}/F_{UIT}$ ratio for DIG ionized by such a population of field OB stars would be closer to that in H II regions. In M51, for example, the large difference between the H II regions and DIG ratios suggests the DIG ratio is low, which in this scenario would imply a field OB star population with a later mean spectral type than in M33. Disentangling this effect from a change in the amount of leakage is not possible with these data, as the two have the same effects on the $F_{H\alpha}/F_{UIT}$ ratio.

3.4. Radial and Surface Brightness Variations

For the following analysis we selected four galaxies in order to make the figures easier to read. Figure 5 shows the $F_{H\alpha}/F_{UIT}$ as a function of Hα surface brightness for H II regions and DIG for four of the galaxies with the best FUV images: M33 (B1), M51, M81, and M101. The ratio is correlated with surface brightness in both environments. In the H II regions, a high $F_{H\alpha}/F_{UIT}$ can arise from either a hotter (*i.e.* younger) stellar population, or

higher extinction. Although there is a trend for the $F_{H\alpha}/F_{UIT}$ to increase with $H\alpha$ surface brightness, the brightest H II regions do not have the highest $F_{H\alpha}/F_{UIT}$ ratios (this is most apparent in M101 or M81, for example). In fact the scatter in the ratio tends to increase as the $H\alpha$ intensity decreases from the brightest to moderately bright regions, so that the regions with the highest $F_{H\alpha}/F_{UIT}$ are only moderately bright regions, while the brightest regions have a more moderate ratio (although less so for M33). This scatter is larger than the uncertainty in the ratio, which even at a very conservative 30% in the low luminosity regions is only about ±0.1 in the logarithmic plot. These high ratios may be caused by undersampling of the IMF in regions with low total mass of stars formed (*e.g.* Oey & Clarke 1998). If the undersampling causes the mass function to be top-heavy (more very massive early O stars and few or no less massive late O and B stars) a high $F_{H\alpha}/F_{UIT}$ ratio will result. Our choice to use the brightest H II regions to define the extinction correction for the histograms in Figures 3 and 4 rather than those with the highest $F_{H\alpha}/F_{UIT}$ ratio was designed to avoid these stochastic effects.

Figure 6 shows the $F_{H\alpha}/F_{UIT}$ ratio as a function of projected distance from the center of the galaxy. The higher ratios in the H II regions are clearly seen again, and several of the galaxies show higher ratios in the DIG toward the center of the galaxy, although it is not apparent in M101. In the total sample about half of the galaxies exhibit this trend. Possibly related to this effect is the fact that the DIG near the centers of spirals is usually brighter than DIG further out (Greenawalt 1998). The radial trend could be an effect of extinction. Higher extinction in the centers of galaxies would produce higher $F_{H\alpha}/F_{UIT}$ ratios.

Figure 7 shows the $F_{H\alpha}/F_{UIT}$ ratio in DIG regions as a function of projected distance from the nearest H II region. In general, it appears that at larger distances from H II regions, the DIG regions have lower $F_{H\alpha}/F_{UIT}$, while near H II regions, the DIG regions can have low or high ratios (*i.e.* , the high ratio DIG regions are missing far from H II regions). A higher $F_{H\alpha}/F_{UIT}$ in the DIG can either mean that the field OB star population there is dominated by earlier-type stars, or it may indicate a larger fraction of leakage of ionizing photons into the region. Both scenarios seem possible near H II regions, and we cannot distinguish between the two with these data. We explore this further in Figure 8, which shows the $F_{H\alpha}/F_{UIT}$ for inter-arm and spiral arm DIG regions in M51. The inter-arm DIG regions generally have lower ratios than spiral arm DIG (with much overlap), but this may just be part of a continuous trend with $H\alpha$ surface brightness. The faintest DIG regions are the inter-arm regions, but whether this is a result of the fewer ionizing photons or less gas to ionize is not clear.

One scenario that could plausibly explain the low $F_{H\alpha}/F_{UIT}$ ratios in the inter-arm DIG is that a lower fraction of the DIG is ionized by leakage in the inter-arm region. In a DIG

region, the field OB stars emit FUV flux and ionizing photons, but there is an extra flux of ionizing photons from outside of the region (leaking into the DIG from an H II region). Reducing this extra component of N_{Lyc} would result in a lower $F_{H\alpha}/F_{UIT}$ ratio. If this is the case in the inter-arm regions, one would expect fainter DIG due to fewer available ionizing photons. One would also expect the field OB stars to also be more sparse in the inter-arm region, further reducing the DIG luminosity.

4.   Discussion and Conclusions

We have compared the FUV and Hα images of 10 nearby spirals in order to investigate the field star populations and their contribution to the ionization of the DIG. We find that the $F_{H\alpha}/F_{UIT}$ ratio is lower in the DIG than in H II regions, an indication that the field OB stars are predominantly later-types. When roughly corrected for extinction and compared to models of evolving stellar populations, we find that the DIG $F_{H\alpha}/F_{UIT}$ most closely resemble a steady-state model, or a burst model at an older age than H II regions. Comparing the difference between the H II region and DIG ratios with that in M33, we find that field OB stars are important contributors to the DIG ionization in most of the galaxies, and in some galaxies they may be the dominant ionization source.

The similarity of the $F_{H\alpha}/F_{UIT}$ in the DIG of the sample of spirals studied here to that of M33 suggests that field OB stars in these galaxies are responsible for a similar fraction of the ionization of the DIG as in M33. Evidence for some variation in this amount is seen, with field stars perhaps dominating the emission in M51 and NGC 628, but contributing relatively little in NGC 1512 and NGC 1313 (but still 15% or more). Most of the galaxies are similar to M33, however, with field OB star contributions around 40%. The variation seen depends on many assumptions, and could be affected by varying extinction, or it could be a result of differences in the mean spectral type of the field star population. As a result, the precise contributions found for each galaxy may not be reliable, and the strongest result is that field OB stars appear to be an important ionization source in all of the galaxies. If the contribution is in fact around 40% for all spirals, this reduces by almost half the amount of leakage required from H II regions to power the DIG. There are indications that other sources such as shock ionization or turbulent mixing layers (Slavin, Shull, & Begelman 1993) contribute as much as 20% of the ionization of the DIG in some galaxies (Greenawalt, Walterbos, & Braun 1997; Wang et al. 1997), further reducing the amount of leakage from H II regions required. In fact, Slavin, McKee, & Holenbach (2000) calculate that cooling supernova remnants may account for 50% of the ionization of the DIG in the Milky Way. The combination of these mechanisms may almost eliminate the need for density-bounded

H II regions.

Elmegreen (1997, 1998) presented a fractal model of the ISM, in which ionizing photons can travel at least twice as far as the Strömgren radius. Leakage of ionizing photons from H II regions is thus expected in this model, and it should have a large effect on the gas near H II regions. It is interesting that we see some indications that the fraction of DIG ionized by leakage may be lower far from H II regions. It seems natural to expect that the DIG near H II regions and in spiral arms is ionized by leakage, and the ionization of the DIG in the inter-arm region has a more important contribution from field OB stars. This scenario can be tested through spectroscopy of the DIG, particularly with the He I 5876Å and [O III] 5007+4959Å lines. These lines both require high energy photons emitted only by the earliest O stars, so they should be strongest in DIG ionized by leakage, since early O stars in H II regions would contribute to the ionizing spectrum. In the field, very early O stars are rare (Massey et al. 1995b; Hoopes & Walterbos 2000), so these line should be weak. We plan to carry out this test in the near future.

The fact that field OB star ionization is viable in this sample of 10 spirals suggests that it may be a common feature of spirals. OB stars outside of H II regions appear to be fairly important in the energy balance of the ISM in spirals then, as the results suggest that at least 15% of the ionizing photons emitted by OB stars are not emitted in H II regions. This fraction may be higher if other sources contribute to the ionization of the DIG. Since they are in the diffuse ISM, the influence of these stars may extend much further than their counterparts in dense H II regions. By ionizing and heating the intercloud medium, they may prevent it from condensing, tempering the formation of molecular clouds, and thus star formation.

There is clearly a difference between the OB stellar population in the field and that in H II regions. The fact that the $F_{H\alpha}/F_{UIT}$ ratios are lower in the DIG in spite of the addition of ionizing photons through leakage from H II regions indicates that later type OB stars dominate in the field. This has bearing on the origin of this population. Since later-type OB stars have longer lives than earlier-types, they are more likely to live long enough to diffuse out of an H II region, or to survive when an H II region is destroyed by SNe from the more massive stars. In this case the mass function of field OB stars would be truncated at the stellar mass whose lifetime corresponds to the time it takes OB stars to become field stars. This time may not be the same for every star formation event, and since the field OB population is probably a mixture if stars from several star formation events, the composite IMF would appear steeper than that for H II regions. Thus while the mass function of the field OB population would be steeper than H II region stars, the *initial* mass function would not. However, if these stars formed in the field, then the paucity of early-type OB stars

suggests that the *initial* mass function is steeper in the field, and that the process of star formation is fundamentally different in the field environment. In Hoopes & Walterbos (2000) and this paper, no distinction could be made between field stars that may have drifted out of H II regions and those that could only have formed in the field. The former category certainly exists, but whether it makes up all or only part of the field OB population is not clear. For LMC field OB stars, Massey et al. (1995b) carefully corrected for stars that were close enough to an H II region to have drifted out, and the mass function was still found to be steeper than in H II regions. Whether these stars may have originated in H II regions that no longer exist is not clear, but is very important in the interpretation of the mass function slope.

REFERENCES

Bell, E. F. & Kennicutt, R. C. 2001, ApJ, 548, 681

Bresolin, F., Kennicutt, R. C., & Stetson, P. B. 1996, AJ, 112, 1009

Buta, R. 1988, ApJS, 66, 233

Cardelli, J. A., Clayton, G. C., & Mathis, J. S. 1989, ApJ, 345, 245

Cornett, R. H. et al. 1994, ApJ, 426, 553

Elmegreen, B. G. 1997, ApJ, 477, 196

Elmegreen, B. G. 1998, PASA, 15, 74

Ferguson, A. M. N., Wyse, R. F. G., Gallagher, J. S., Hunter, D. A. 1996, AJ, 111, 2265

Galarza, V. C., Walterbos, R. A. M., & Braun, R. 1999, AJ, 118, 2775

Greenawalt, B. 1998, Ph.D. Thesis, New Mexico State University

Greenawalt, B., Walterbos, R. A. M., & Braun, R. 1997, ApJ, 483, 666

Greenawalt, B., Walterbos, R. A. M., Thilker, D. A., & Hoopes, C. G. 1998, ApJ, 506, 135

Haffner, L. M., Reynolds, R. J., & Tufte, S. L. 1999, ApJ, 523, 223

Heiles, C., Koo, B., Levenson, N. A. & Reach, W. T. 1996, ApJ, 462, 326

Hill, J. K. et al. 1995, ApJ, 438, 181

Hill, R. S. et al. 1998, ApJ, 507, 179

Hoopes, C. G. & Walterbos, R. A. M. 2000, ApJ, 541, 597

Hoopes, C. G., Walterbos, R. A. M., & Greenawalt, B. 1996, AJ, 112, 1429

Howarth, I. D. 1983, MNRAS, 203, 301

Jones, A. P., Tielens, A. G. G. M. & Hollenbach, D. J. 1996, ApJ, 469, 740

Kaufman, M., Bash, F. N., Kennicutt, R. C., & Hodge, P. W. 1987, ApJ, 319, 61

Leitherer, C., Schaerer, D. Goldader, J. D., González Delgado, R. M., Robert, C., Foo Kune, D., de Mello, D. F., Devost, D., & Heckman, T. M. 1999, ApJS, 123, 3

Massey, P. 1985, PASP, 97, 5

Massey, P. 1998, in ASP Conf. Proc. 142, The Stellar Initial Mass Function, ed. G. Gilmore & D. Howell (San Francisco:ASP), 17

Massey, P., Armandroff, T. E., Pyke, R., Patel, K., & Wilson, C. D. 1995a, AJ, 110, 2715

Massey, P., Lang, C. C., DeGioia-Eastwood, K., & Garmany, C. D. 1995b, ApJ, 438, 188

McKee, C. F. & Williams, J. P. 1997, ApJ, 476, 144

Oey, M. S. & Kennicutt, R. C. 1997, MNRAS, 291, 827

Oey, M. S. & Clarke, C. J. 1998, AJ, 115, 1543

Osterbrock, D. E. 1989, Astrophysics of Gaseous Nebulae and Active Galactic Nuclei (Mill Valley: University Science Books)

Patel, K., & Wilson, C. D. 1995, ApJ, 451, 607

Petersen, L. & Gammelgaard, P. 1996, A&A, 308, 49

Rand, R. J. 1997, ApJ, 474, 129

Quillen, A. C. & Yukita, M. 2001, AJ, 121, 2095

Reynolds, R. J. 1991, in The Interstellar Disk-Halo Connection in Galaxies, IAU Symposium No. 144, edited by H. Bloemen (Dordrecht:Kluwer), 67

Reynolds, R. J. & Tufte, S. L. 1995, ApJ, 439, L17

Roy, J. & Walsh, J. R. 1986, MNRAS, 223, 39

Schaerer, D. & de Koter, A. 1997, A&A, 322, 598

Schaerer, D., Meynet, G., Maeder, A., & Schaller, G. 1993, A&AS, 98, 523

Slavin, J. D., McKee, C. F., & Hollenbach, D. J. 2000, ApJ, 541, 218

Slavin, J. D., Shull, J. M., & Begelman, M. C. 1993, ApJ, 407, 83

Stecher, T., et al. 1997, PASP, 109, 584

Stewart, S. G., et al. 2000, ApJ, 529, 201

Torres-Peimbert, S., Lazcano-Araujo, A., & Peimbert, M. 1974, ApJ, 191, 401

von Hippel, T., & Bothun, G. 1990, AJ, 100, 403

Walterbos, R. A. M., & Braun, R. 1994, ApJ, 431, 156

Walterbos, R. A. M., & Braun, R. 1996, in ASP Conf. Proc. 106, The Minnesota Lectures on Extragalactic Neutral Hydrogen, ed. E. D. Skillman (San Francisco:ASP), 1

Walsh, J. R. & Roy, J. -. 1997, MNRAS, 288, 726

Wang, J., Heckman, T. M., & Lehnert, M. D. 1997, ApJ, 491, 114

Zaritsky, D., Kennicutt, R. C., & Huchra, J. P. 1994, ApJ, 420, 87

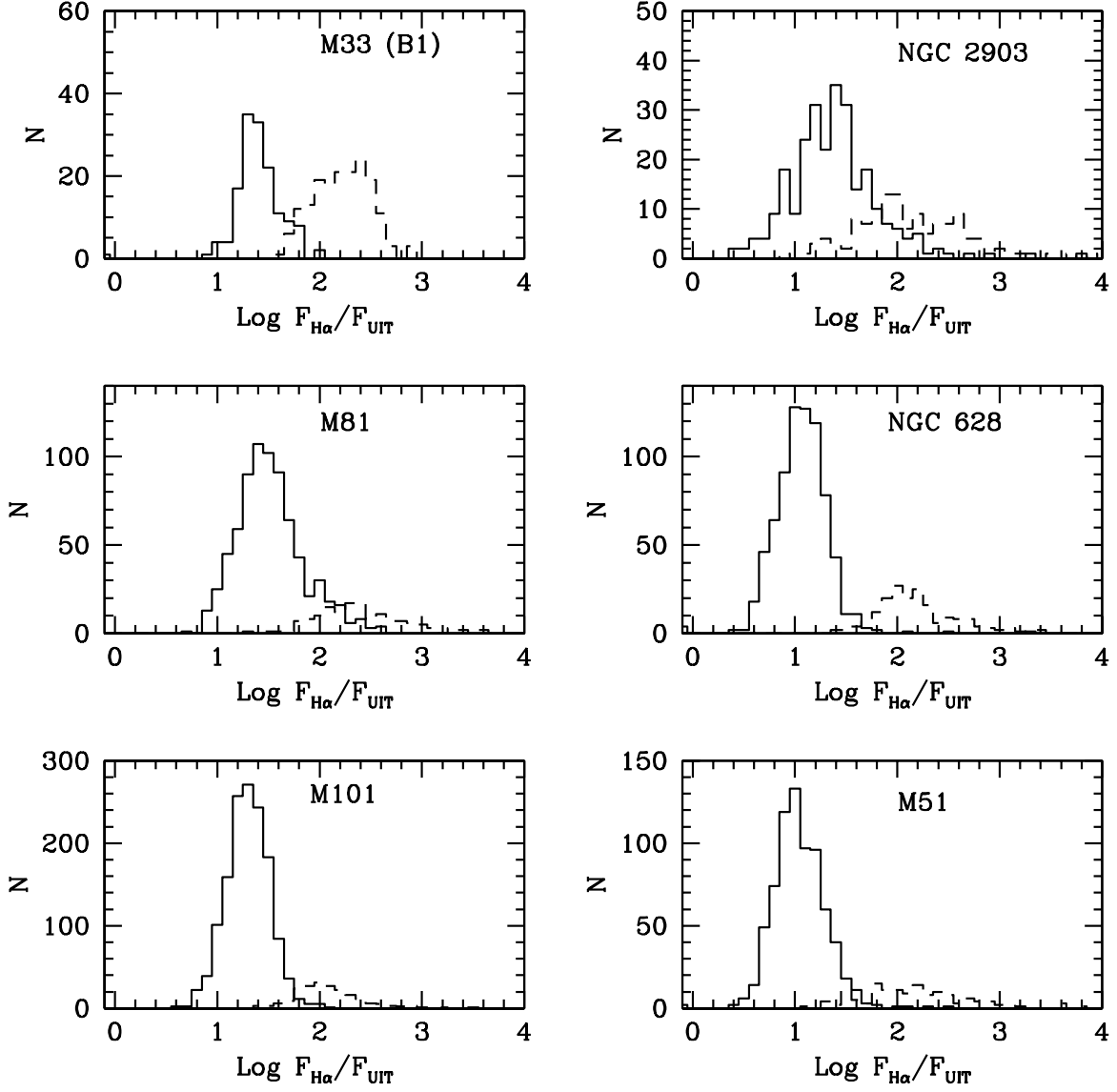Fig. 1.— Histograms of the $F_{H\alpha}/F_{UIT}$ ratios for the galaxies observed through the B1 filter. H II regions are shown with a dashed line, and DIG with a solid line. These histograms have not been corrected for extinction.
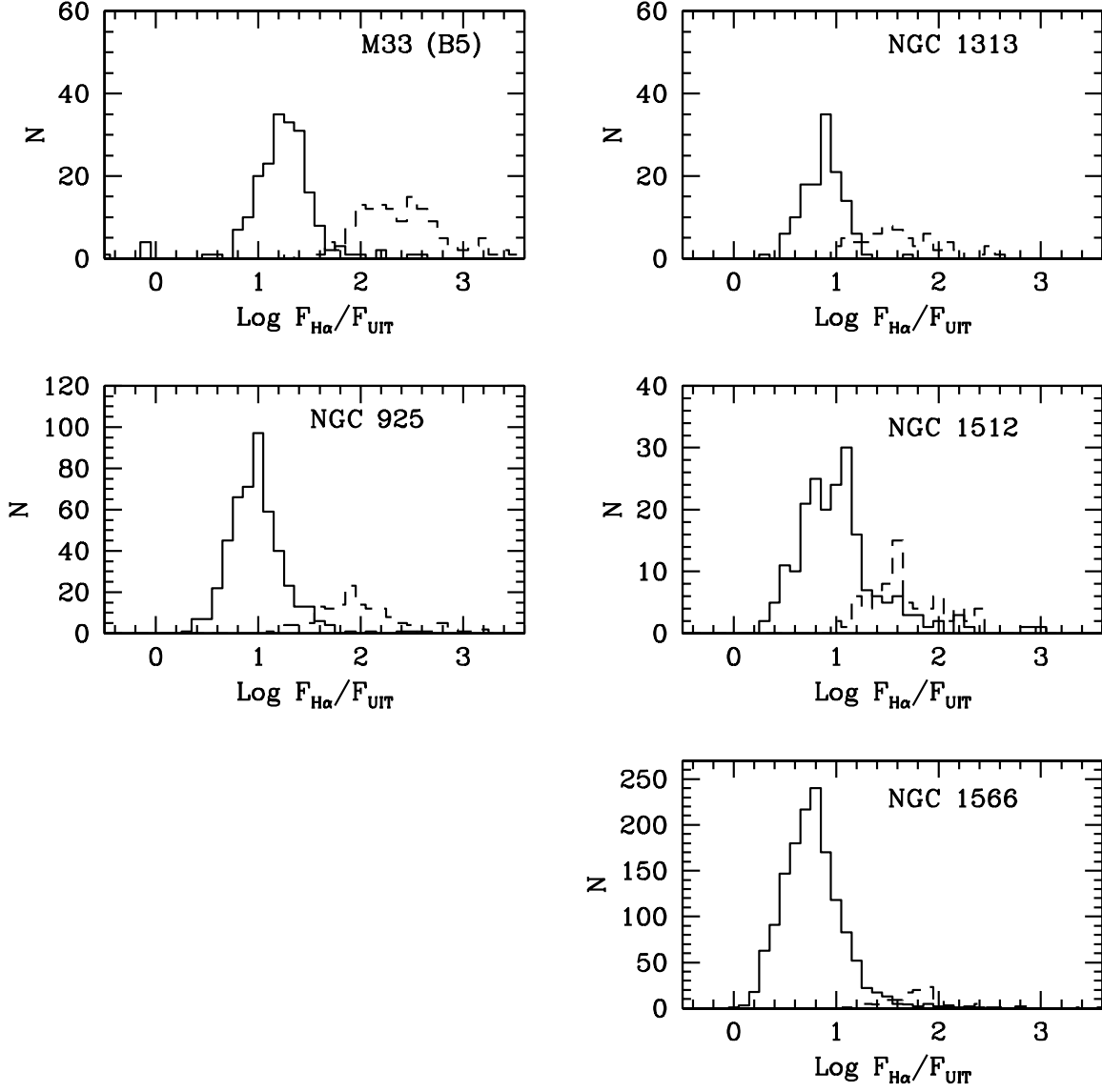
Fig. 2.— Histograms of the $F_{H\alpha}/F_{UIT}$ ratios for the galaxies observed through the B5 filter. H II regions are shown with a dashed line, and DIG with a solid line. These histograms have not been corrected for extinction.
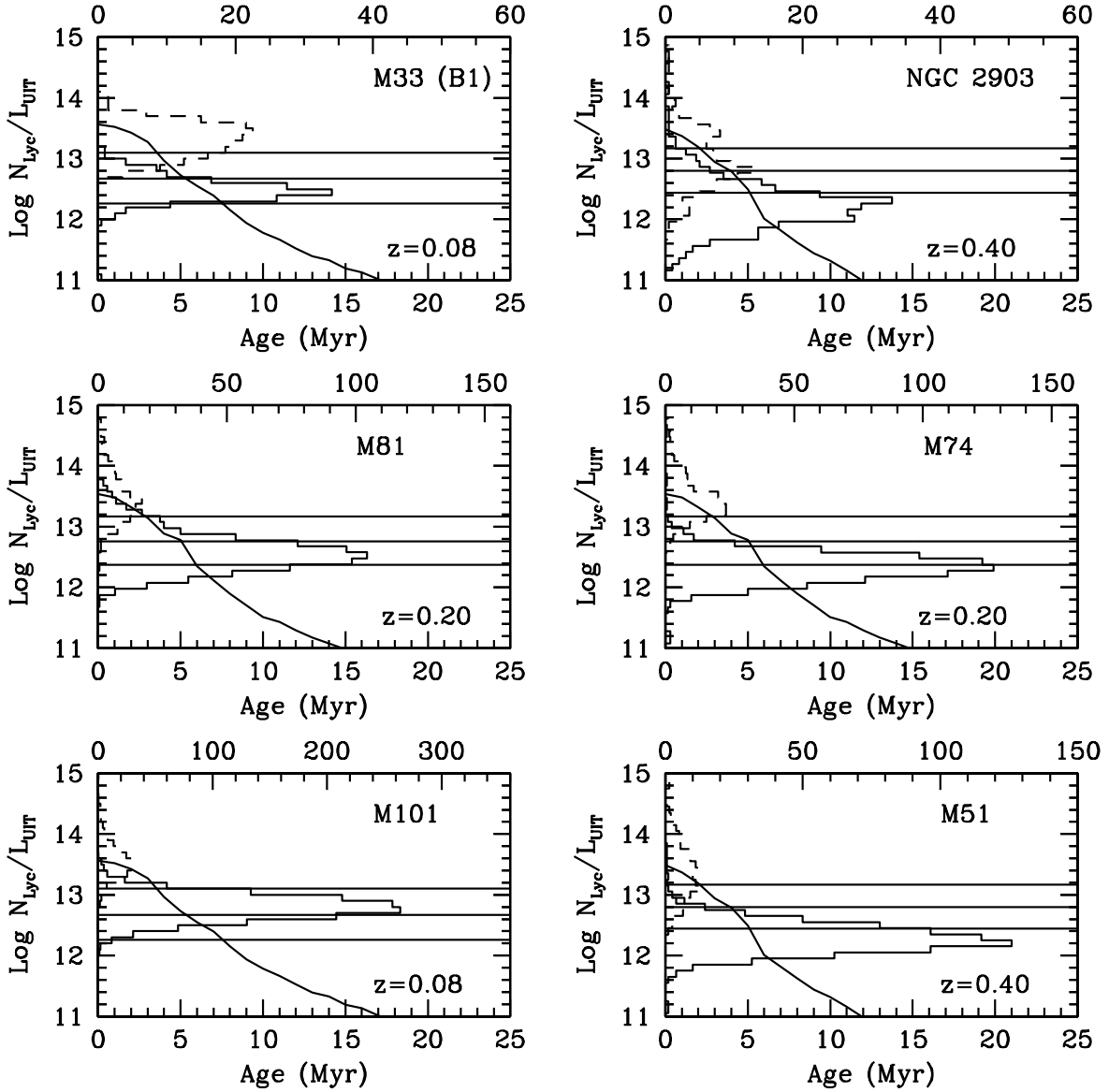
Fig. 3.— Histograms of the N_{Lyc}/L_{UIT} ratios for the galaxies observed through the B1 filter. H II regions are shown with a dashed line, and DIG with a solid line. Starburst99 (Leitherer et al. 1999) models are also shown. The falling line is a single burst model, and the horizontal lines are the equilibrium values of steady state models with constant star formation. The IMF slopes were used in the steady state models, α=2.35 (top line), α=3.00 (middle line), and α=3.5 (bottom line). The metallicity of the models for each galaxy is given in the figure. The histograms have been corrected for extinction by shifting the H II regions to match the models, as described in the text.

Fig. 4.— Histograms of the N_{Lyc}/L_{UIT} ratios for the galaxies observed through the B5 filter. H II regions are shown with a dashed line, and DIG with a solid line. Starburst99 (Leitherer et al. 1999) models are also shown. The falling line is a single burst model, and the horizontal lines are the equilibrium values of steady state models with constant star formation. The IMF slopes were used in the steady state models, α=2.35 (top line), α=3.00 (middle line), and α=3.5 (bottom line). The metallicity of the models for each galaxy is given in the figure. The histograms have been corrected for extinction by shifting the H II regions to match the models, as described in the text.
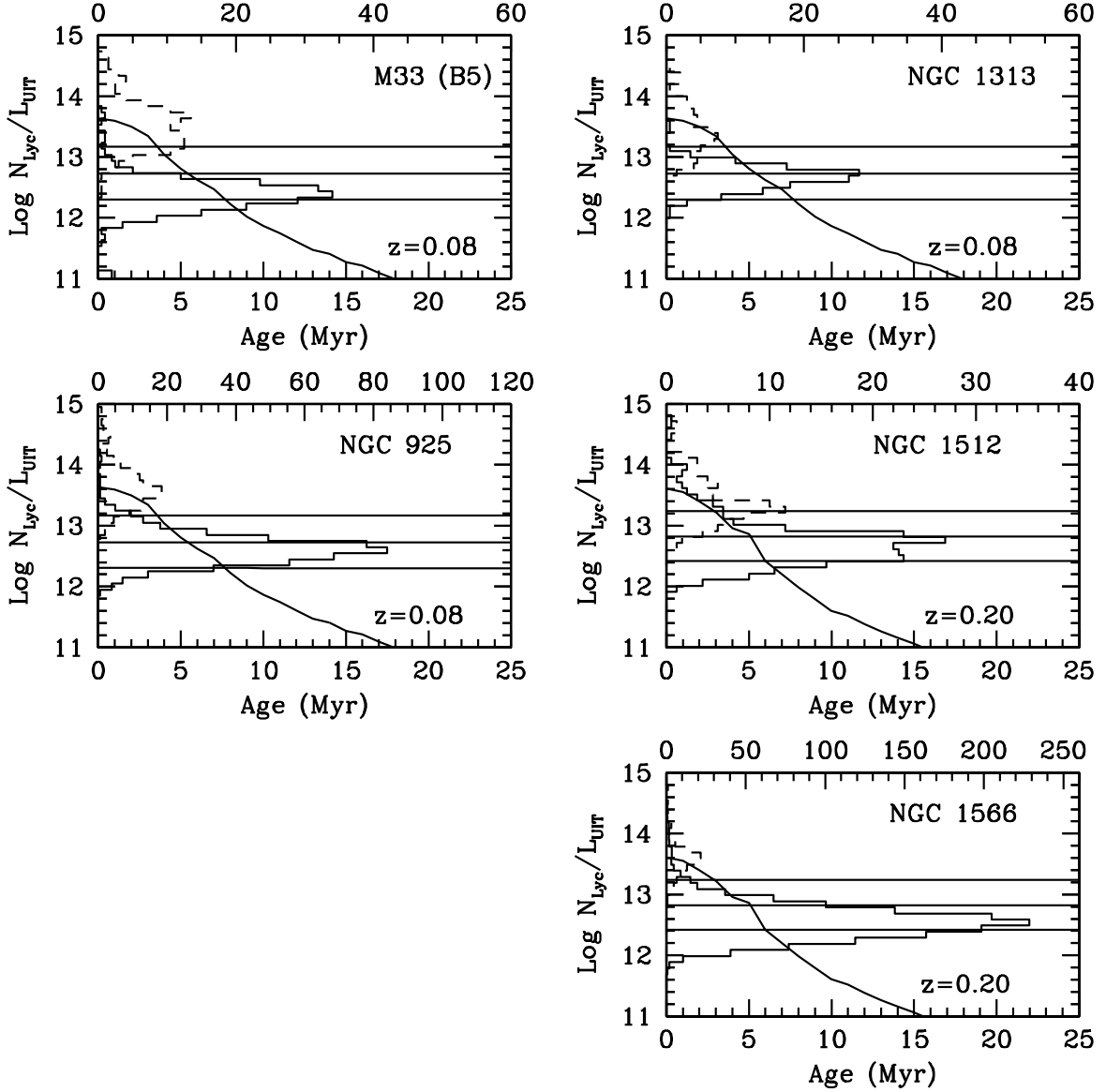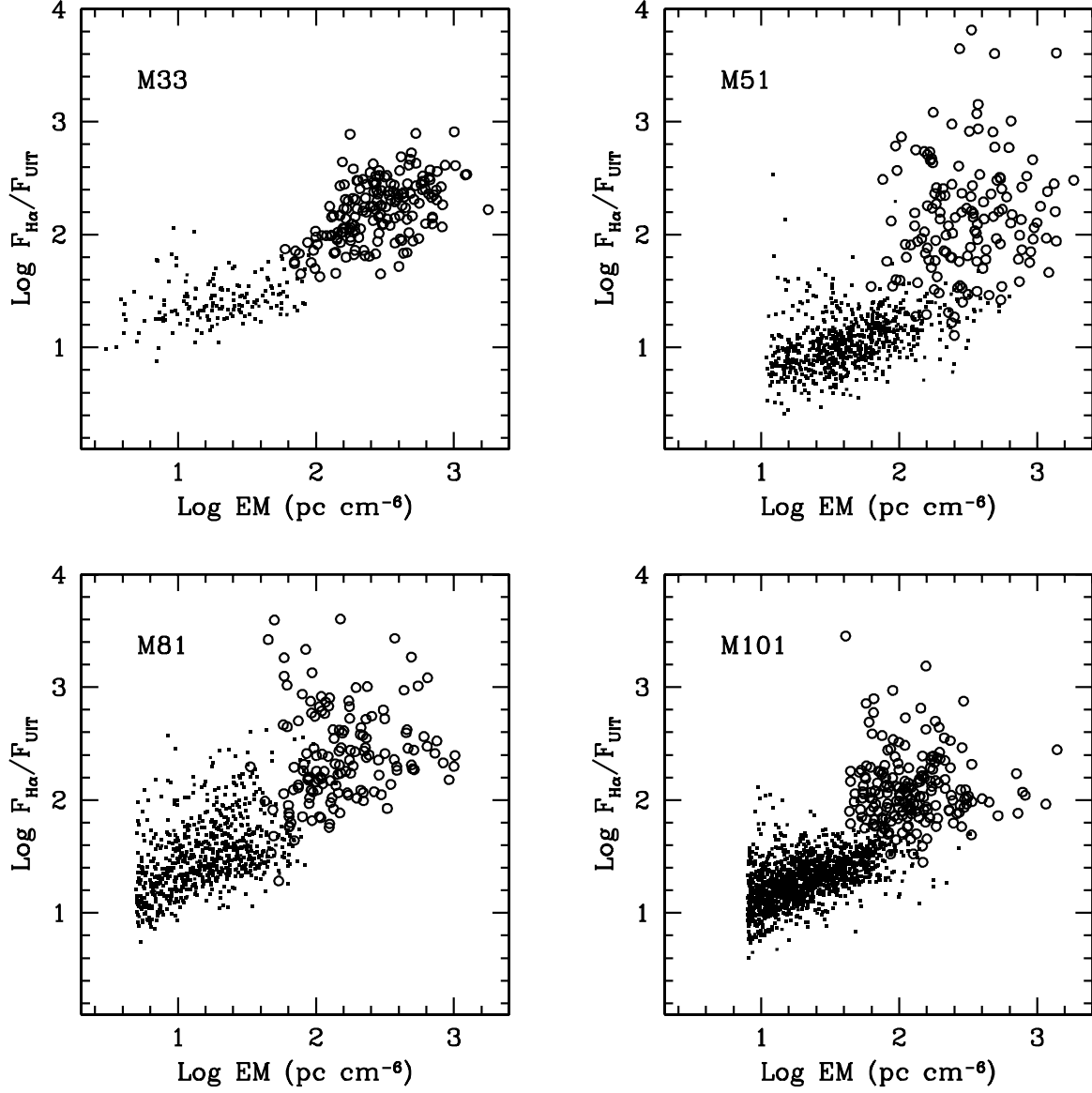
Fig. 5.— The $F_{H\alpha}/F_{UIT}$ ratio as a function of Hα surface brightness. H II regions are shown as open circles, and the crosses are DIG regions. The low surface brightness cutoff is defined by the sensitivity of the Hα image. The ratios were not corrected for extinction.
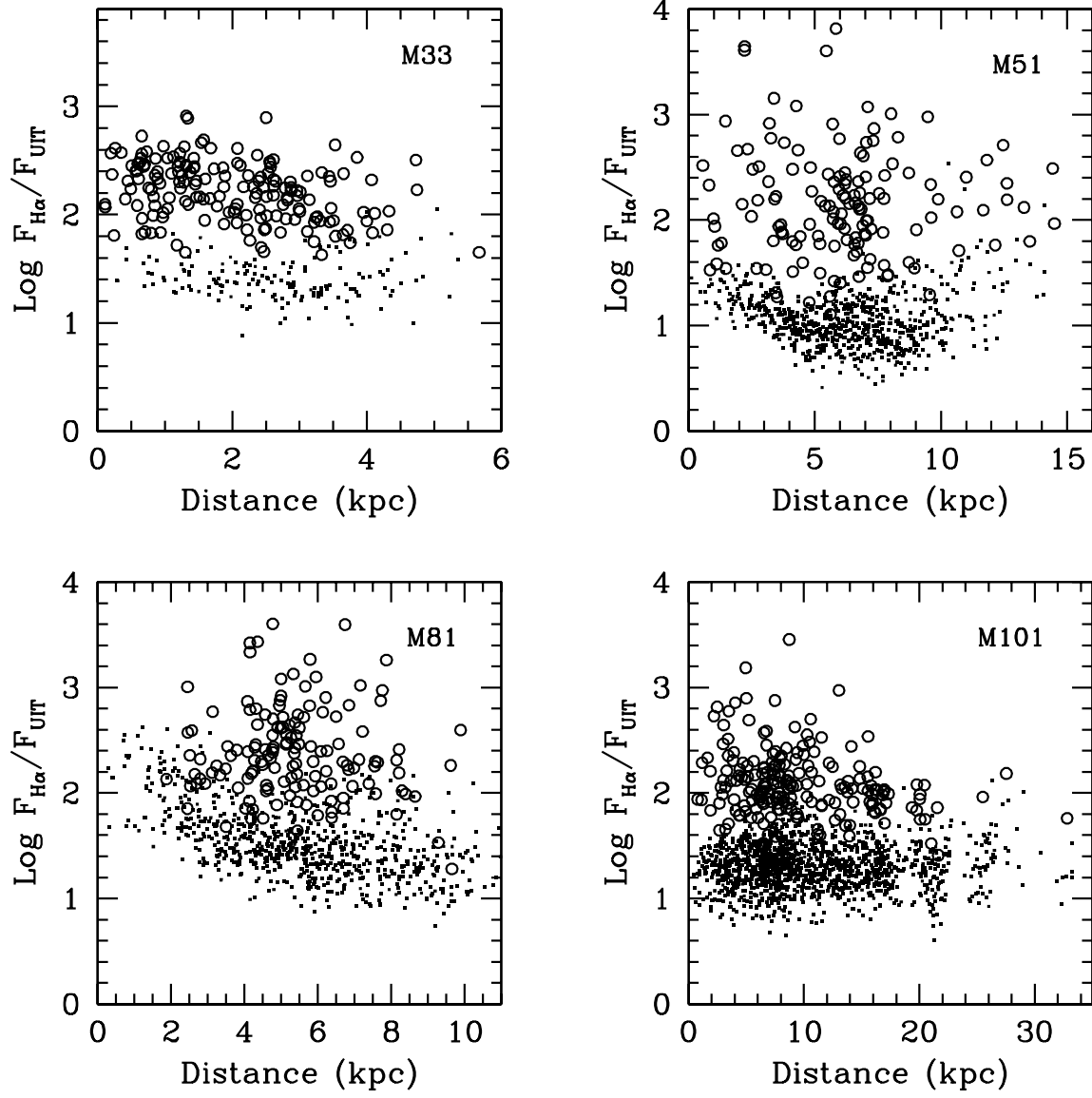
Fig. 6.— The $F_{H\alpha}/F_{UIT}$ ratio as a function of projected galactocentric distance in four galaxies. H II regions are shown as open circles, and the points are DIG regions. The ratios were not corrected for extinction.

Fig. 7.— The $F_{H\alpha}/F_{UIT}$ ratio in the DIG regions as a function of the projected distance from the nearest H II region in four galaxies. Some points have a distance of zero because there is an H II region in the DIG box (DIG fluxes were measured on images with the H II regions masked out). The ratios were not corrected for extinction.

Fig. 8.— The $F_{H\alpha}/F_{UIT}$ ratio as a function of Hα surface brightness for M51 DIG points. The open circles are spiral arm DIG regions, and the crosses are inter-arm DIG regions. The ratios were not corrected for extinction.

Table 1.   Galaxy Sample

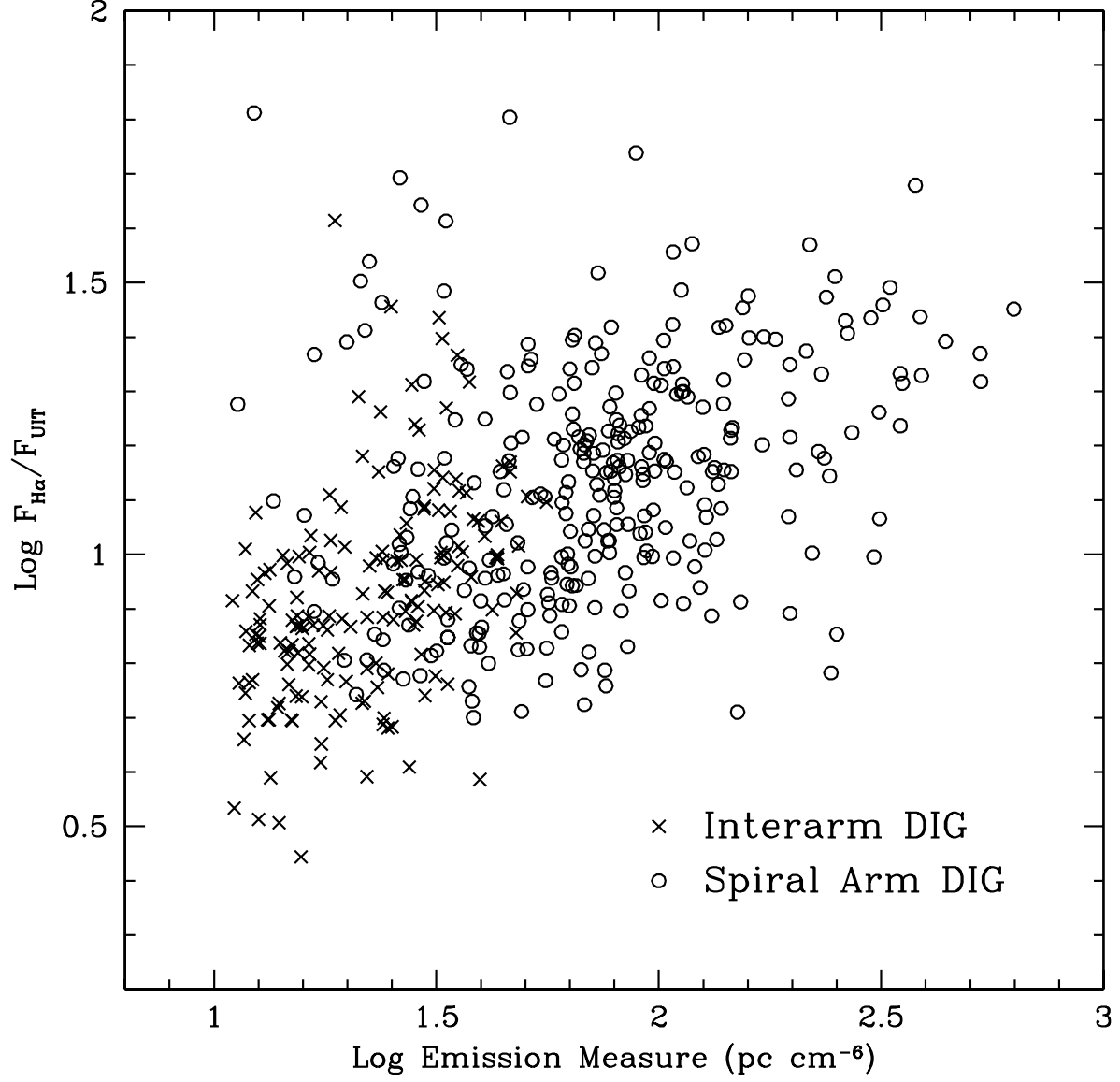| Galaxy	Distance (Mpc)	Hubble Type	12+log(O/H)[a]
NGC 598 (M33)	0.84	Scd	8.70±0.06
NGC 628 (M74)	9.7	Sc	9.13±0.16
NGC 925	9.3	Sd	8.68±0.11
NGC 1313	4.5	SBd	8.33±0.11
NGC 1512	16.6[b]	SBa	$\cdots$
NGC 1566	17.4	Sbc	9.10±0.40
NGC 2903	6.3	Sbc	9.22±0.07
NGC 3031 (M81)	3.6	Sab	8.89±0.16
NGC 5194 (M51)	9.6	Sbc	9.28±0.11
NGC 5457 (M101)	7.4	Scd	8.76±0.05

[a]Oxygen abundance at 3 kpc radius, from Zaritsky et al. 1994. The metallicity of NGC 1512 was not found in the literature.

[b]The distance to NGC 1512 is uncertain. This value was taken from Buta (1988).

Table 2.   Hα Data

Galaxy	Hα Telescope	Hα Exposure Time (seconds)	Hα Sensitivity[a]	Hα Calibration
NGC 598 (M33)	KPNO Schmidt	20×900	0.8	R-mag
NGC 628 (M74)	KPNO 0.9m	16×900	0.9	Standard
NGC 925	KPNO 0.9m	16×900	1.3	Standard
NGC 1313	CTIO 0.9m	2×900	2.2	Standard
NGC 1512	CTIO 0.9m	2×1400	1.6	Standard
NGC 1566	CTIO 0.9m	2×1000	1.4	Standard
NGC 2903	KPNO 0.9m	16×900	0.7	Standard
NGC 3031 (M81)	KPNO Schmidt	14×900	1.5	H II Regions
NGC 5194 (M51)	KPNO 0.9m	3×1200	2.7	R-mag
NGC 5457 (M101)	KPNO Schmidt	13×900	1.6	H II Regions

[a]$\times 10^{17}$erg s^{-1} cm^{-2} arcsec^{-2}

Table 3.   UIT Data

Galaxy	Exposure Time (seconds)	Filter[a]	Sensitivity[b]	Resolution[c] (parsecs)	Mission
NGC 598 (M33)	424	B1	1.3	8	Astro-1
NGC 598 (M33)	626	B5	2.0	8	Astro-2
NGC 628 (M74)	514	B1	0.9	70	Astro-1
NGC 925	1590	B5	0.7	90	Astro-2
NGC 1313	1070	B5	1.0	44	Astro-2
NGC 1512	948	B5	1.1	161	Astro-2
NGC 1566	1390	B5	0.8	169	Astro-2
NGC 2903	548	B1	1.0	61	Astro-2
NGC 3031 (M81)	640	B1	0.8	35	Astro-1
NGC 5194 (M51)	1100	B1	0.5	93	Astro-2
NGC 5457 (M101)	1310	B1	0.5	72	Astro-2

[a]The UIT B1 filter is 354Å wide with an effective wavelength of λ_{eff}=1521Å, and the B5 filter is 225Å wide with λ_{eff}=1615Å.

[b]$\times 10^{17}$erg s^{-1} cm^{-2} arcsec^{-2}

[c]Spatial resolution based on $2''$ angular resolution of UIT.

Table 4.   Measured Properties

Galaxy	$L_{H\alpha}$[a] (erg s^{-1})	Hα DF[a]	log $L_{H\alpha}/L_{UIT}$ Total	log $L_{H\alpha}/L_{UIT}$ H II	log $L_{H\alpha}/L_{UIT}$ DIG	FUV DF[b]
NGC 598 (B1)	$3.0\pm0.3\times10^{40}$	0.38±0.03	1.75±0.10	2.06±0.07	1.47±0.10	0.73±0.21
NGC 628	$1.7\pm0.3\times10^{41}$	0.43±0.05	1.64±0.11	2.41±0.09	1.31±0.11	0.91±0.26
NGC 2903	$6.5\pm1.8\times10^{40}$	0.27±0.09	2.16±0.14	2.54±0.12	1.74±0.14	0.72±0.21
NGC 3031	$7.8\pm1.2\times10^{40}$	0.49±0.08	2.12±0.11	2.65±0.08	1.87±0.11	0.87±0.25
NGC 5194	$3.1\pm0.3\times10^{41}$	0.43±0.03	1.88±0.10	2.22±0.07	1.62±0.10	0.77±0.22
NGC 5457	$2.4\pm0.3\times10^{41}$	0.43±0.04	1.41±0.11	1.95±0.08	1.11±0.11	0.84±0.24
NGC 598 (B5)	$3.0\pm0.3\times10^{40}$	0.38±0.03	1.51±0.10	1.99±0.07	1.17±0.10	0.84±0.24
NGC 925	$7.6\pm0.5\times10^{40}$	0.37±0.05	1.70±0.10	2.30±0.06	1.33±0.10	0.86±0.25
NGC 1313	$2.7\pm0.5\times10^{40}$	0.46±0.09	1.57±0.12	1.88±0.09	1.35±0.12	0.76±0.22
NGC 1512	$2.9\pm0.6\times10^{40}$	0.15±0.03	1.25±0.12	2.20±0.10	0.47±0.12	0.91±0.26
NGC 1566	$3.2\pm0.6\times10^{41}$	0.33±0.07	1.58±0.12	2.13±0.09	1.18±0.12	0.82±0.23

[a]The Hα filter used for NGC 3031, NGC 5194, and NGC 5457 contains a contribution from [N II].

[b]The diffuse fraction (DF) is the ratio of the luminosity contributed by DIG to the total luminosity of the galaxy.

Table 5.   Extinction Corrections

Galaxy	Mean Observed Log N_{Lyc}/L_{UIT}	Difference[a]	E(B-V) MW[b]	E(B-V) LMC[b]	Published E(B-V)[c]
NGC 598 (B1)	14.27	0.75	0.33	0.23	$0.05 - 0.33$
NGC 628	14.05	0.57	0.25	0.18	$0.47 - 0.52$
NGC 2903	14.35	0.98	0.44	0.31	$0.68 - 1.34$
NGC 3031	14.25	0.77	0.34	0.24	$0.14 - 0.48$
NGC 5194	13.96	0.59	0.27	0.19	$0.48 - 1.62$
NGC 5457	13.87	0.35	0.15	0.11	$0.00 - 0.40$
NGC 598 (B5)	14.31	0.71	0.33	0.23	$0.05 - 0.33$
NGC 925	13.79	0.20	0.09	0.07	$0.16 - 0.48$
NGC 1313	13.65	0.05	0.02	0.02	$0.31 - 0.83$
NGC 1512	13.68	0.13	0.06	0.04	$0.18 - 1.06$
NGC 1566	13.61	0.06	0.03	0.02	$0.55 - 0.74$

[a]The difference between the observed Log N_{Lyc}/L_{UIT} and that predicted for a 1 Myr burst.

[b]The amount of extinction which would account for the difference. The Milky Way extinction law is from Cardelli et al. 1989, and the LMC extinction law is from Howarth 1983.

[c]References for published reddening: NGC 598 – Massey et al. 1995a; NGC 628 – Petersen & Gammelgaard 1996; NGC 2903, NGC 1512, NGC 5194 – Quillen & Yukita 2001; NGC 3031 – Kaufman et al. 1987; NGC 5457 – Bresolin, Kennicutt, & Stetson 1996; NGC 925 – Zaritsky et al. 1994; NGC 1313 – Walsh & Roy 1997; NGC 1566 – Roy & Walsh 1986 (c(Hβ) was converted to E(B-V) for NGC 1566).

Table 6.   Galaxy Comparison

Galaxy	Log (mean $F_{H\alpha}/F_{UIT}$) HII $-$ Log (mean $F_{H\alpha}/F_{UIT}$) DIG	Fraction of M33 Ratio	Field Star Contribution (%)
NGC 598 (B1)	0.81±0.10	$\cdots$	0.40±0.12[a]
NGC 628	1.17±0.11	0.44±0.17	0.91±0.17
NGC 2903	0.73±0.14	1.20±0.55	0.33±0.19
NGC 3031	0.87±0.11	0.87±0.34	0.46±0.21
NGC 5194	1.09±0.10	0.52±0.20	0.77±0.22
NGC 5457	0.78±0.11	1.07±0.41	0.37±0.17
NGC 598 (B5)	1.16±0.10	$\cdots$	0.40±0.12[a]
NGC 925	1.02±0.10	1.38±0.52	0.29±0.13
NGC 1313	0.81±0.12	2.24±0.92	0.18±0.09
NGC 1512	0.72±0.12	2.75±1.15	0.15±0.08
NGC 1566	1.13±0.12	1.07±0.44	0.37±0.18

[a]The field OB star contribution given for M33 was that measured in Hoopes & Walterbos 2000.